Static and dynamical magnetic properties of the itinerant ferromagnet $LaCo_2P_2$

Masaki Imai,[1,*] Chishiro Michioka,[1] Hiroaki Ueda,[1] and Kazuyoshi Yoshimura[1,2,†]
[1]*Department of Chemistry, Graduate School of Science, Kyoto University, Kyoto 606-8502, Japan*
[2]*Research Center for Low Temperature and Materials Sciences, Kyoto University, Kyoto 606-8501, Japan*

(Received 12 February 2015; revised manuscript received 21 April 2015; published 26 May 2015)

We synthesized single crystals of an itinerant ferromagnet $LaCo_2P_2$ with $ThCr_2Si_2$-type structure and studied their magnetism by magnetization and ^{31}P NMR measurements. We measured Knight shift K and spin-lattice relaxation rate divided by temperature $1/T_1T$ with the applied fields parallel to the a and c axes, and estimated spin fluctuations in the ab plane and c. In addition, we evaluated spin fluctuations from the result of magnetization data with a three-dimensional ferromagnetic model. There is little anisotropy in evaluated spin fluctuations in the ab plane and c. Spin fluctuations of $LaCo_2P_2$ have a three-dimensional character and can be understood in the framework of the self-consistent renormalization theory of spin fluctuations.

DOI: 10.1103/PhysRevB.91.184414 PACS number(s): 76.60.−k, 75.40.Gb

I. INTRODUCTION

Since the discovery of iron-based high-T_c superconductors, the layered transition metal compounds have been intensively studied in the investigation field of strongly correlated electron systems. The $ThCr_2Si_2$-type layered compounds $AT_2Pn_2(A =$ alkali metals, alkaline earth metals, lanthanoids, $T =$ transition metals, $Pn =$ pnictogens) with space group $I4/mmm$ exhibit a wide variety of physical properties, such as high-T_c superconductivity in the iron-based system [1–4]. In these compounds, because edge-shared TPn tetrahedral layers and A layers stack alternately, interactions are expected to be strongly held in the quasi-two-dimensional TPn layer. The iron pnictide system has an antiferromagnetic interaction in the TPn layer, and its superconductivity appears in the vicinity of the antiferromagnetic quantum critical point similar to the high-T_c cuprates and heavy-fermion superconductors [5–8]. Investigations of their quantum critical phenomena have been greatly contributed to clarify the mechanism of superconductivity. Although such investigations are powerfully carried out in antiferromagnetic cases, only a few novel phase transitions are discovered in ferromagnetic cases.

In the above situation, the ACo_2P_2 compounds with a ferromagnetic interaction in a CoP layer oppositely to the iron-based superconductors can be regarded as an adequate system [9,10]. $SrCo_2P_2$ shows no magnetic ordering among the ACo_2P_2 compounds, even though its CoP layer has the ferromagnetic interaction [2,11]. We discovered an itinerant-electron metamagnetic transition of $SrCo_2P_2$, in which a Pauli paramagnetic ground state turns into a ferromagnetic one under the high magnetic field [11]. Here, we present dynamical magnetic properties of the itinerant ferromagnetic compound $LaCo_2P_2$, in which the ferromagnetic ground state is driven by a similar magnetic interaction, by the nuclear magnetic resonance (NMR) method. Among AT_2P_2, only $LaCo_2P_2$ shows a ferromagnetic ordering without the applied magnetic field. Characterization of the dispersion relation of spin fluctuations has great significance to classify its itinerant ferromagnetism. According to the self-consistent renormalization (SCR) theory of ferromagnetic spin fluctuations, the magnetic susceptibility shows the Curie-Weiss behavior, and the Weiss temperature is regarded as a scaling parameter for the distance from the quantum critical point [12,13]. The Weiss temperature θ has a negative value in the paramagnetic region, and it approaches to 0 as the system comes close to the quantum critical point. Indeed, exchange-enhanced paramagnetic $SrCo_2P_2$ has a negative θ and ferromagnetic $LaCo_2P_2$ a positive θ. Spin fluctuations in an itinerant-electron magnet are related to the dynamical susceptibility which can be directly observed by inelastic neutron diffraction and NMR measurements.

In this paper, we present microscopic magnetic properties of single crystals of $LaCo_2P_2$. We have grown pure single crystals of $LaCo_2P_2$ and studied anisotropy of the magnetism, including details of spin fluctuations by ^{31}P NMR measurements. We analyzed NMR results by using SCR theory and estimated the spin-fluctuation parameters which characterize dynamical susceptibility spreading in the wave number q space and the frequency ω space. In the ferromagnetic case, some of the SCR parameters can be also estimated from the static magnetizations through the SCR equations [12]. We cross-checked their parameters obtained from macroscopic and microscopic measurements and properly evaluated these parameters. We also compared dynamical magnetic properties with those estimated from the SCR theory taking dimensionality into account, and discuss the universality of the ferromagnet $LaCo_2P_2$.

II. EXPERIMENTAL METHOD

Single crystals of $LaCo_2P_2$ with space group $I4/mmm$ were grown by a tin flux method, and powder samples were prepared with solid-state reactions. Single crystals are platelike along the tetragonal ab plane. A powder sample was pulverized to a fine powder in a mortar and aligned along the c axis with an external magnetic field of 5 T at 300 K and fixed in Stycast 1266 epoxy. A crystalline orientation axis was determined by x-ray diffraction. The aligned sample was measured in Bragg-Brentano geometry. Only $00l$ Bragg peaks were observed in diffraction patterns when the applied field direction was parallel to the scattering vector, suggesting the c-axis alignment. The temperature and magnetic-field-dependent magnetizations M of single crystals of $LaCo_2P_2$

*m.imai@kuchem.kyoto-u.ac.jp
†kyhv@kuchem.kyoto-u.ac.jp

were measured by using a Quantum Design MPMS-XL system at the Research Center for Low Temperature and Materials Sciences, Kyoto University. With the magnetic field H applied along the a or c axis, the M vs H curves were measured with decreasing H from 7 to 0 T. Field-swept and Fourier transform (FT) ^{31}P NMR spectra were measured by the spin-echo method by using a standard phase coherent-type spectrometer. The ^{31}P nucleus has a nuclear spin $I = 1/2$ and a gyromagnetic ratio $^{31}\gamma = 17.237$ MHz/T. The shift ^{31}K is defined as $^{31}K = (H_{\rm ref} - H_{\rm obs})/H_{\rm obs}$ or $^{31}K = (\nu_{\rm obs} - \nu_{\rm ref})/\nu_{\rm ref}$, where $H_{\rm ref} = \nu_{\rm ref}/^{31}\gamma$ with the operating frequencies $\nu_{\rm ref}$ of 15.120 or 29.800 MHz and the operating field $H_{\rm ref}$ of 1.217 T, and $H_{\rm obs}$ and $\nu_{\rm obs}$ are the observing field and frequency, respectively. In the paramagnetic region, the shift corresponds to the Knight shift. The nuclear-spin-lattice relaxation time T_1 was measured by the inversion-recovery method for the echo signal after an inversion π pulse. The nuclear magnetization recovery was found to follow a simple single exponential function at the whole temperature region.

III. RESULTS AND DISCUSSION

The temperature and magnetic-field-dependent magnetization of $LaCo_2P_2$ is shown in Fig. 1. The large anisotropy between the directions of the applied fields appears in the ferromagnetic region because of the moments aligned along the a axis. According to Landau theory, the free energy F can be expressed as the expansion of an order parameter. The spontaneous magnetization M is the order parameter in the ferromagnetic case. Thus the free energy $F(M)$ is explained as $F(M) = F_0 + aM^2 + bM^4 + cM^6 + \cdots + MH$. When the sixth and higher terms of M are neglected, the Arrott plots

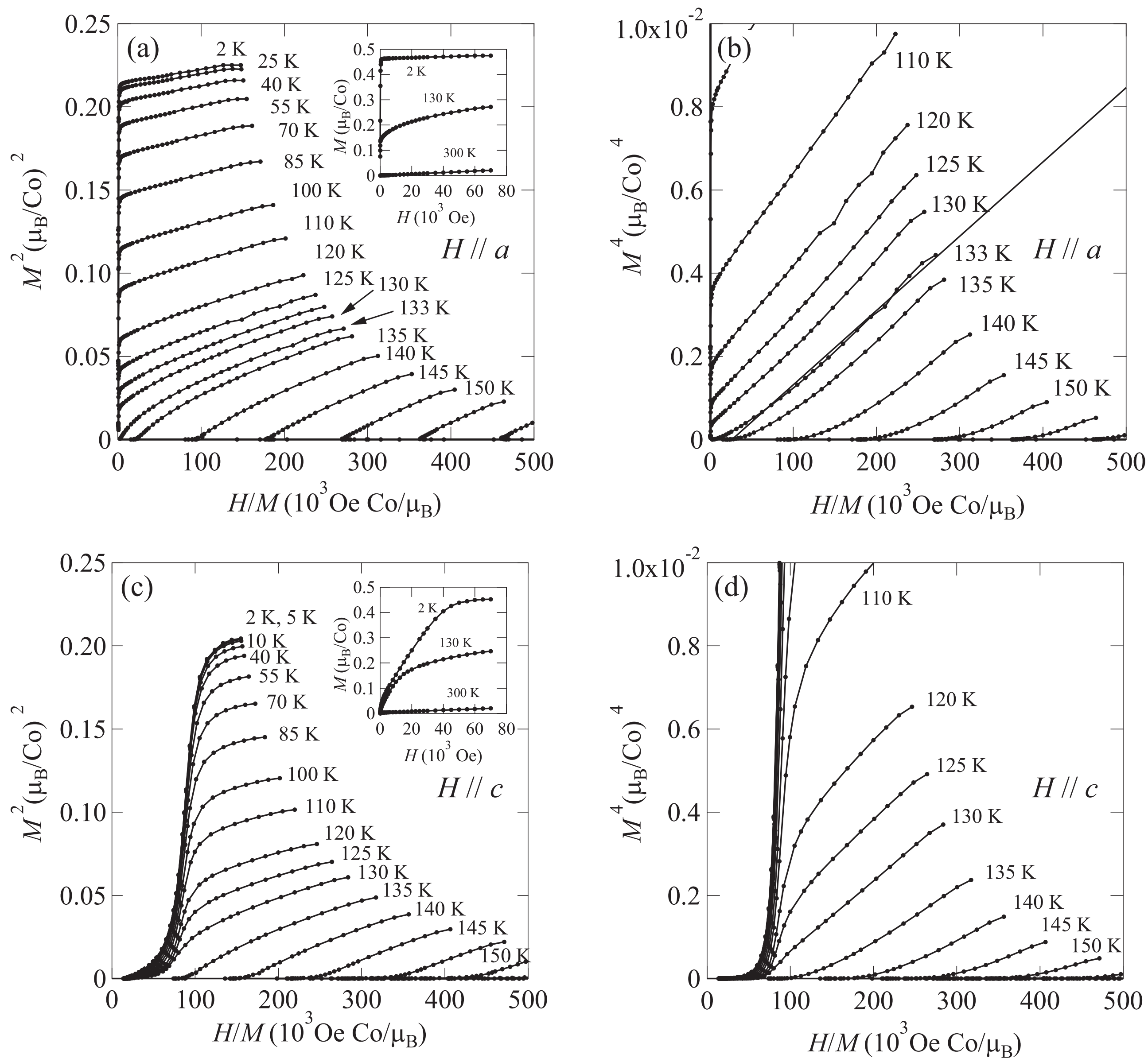

FIG. 1. Temperature and field dependence of magnetization $M(T,H)$ of $LaCo_2P_2$ for $H \parallel a$ and $H \parallel c$. (a) and (b) are Arrott plots (M^2 vs H/M plots) and M^4 versus H/M plots for $H \parallel a$, respectively. (c) and (d) are Arrott plots and M^4 versus H/M plots for $H \parallel c$, respectively. Insets in (a) and (c) show magnetization M vs field H.

[$M^2(T,H)$ vs $H/M(T,H)$ plots] would show good linearity. As shown in Fig. 1(a), a good linear behavior is realized only at low temperatures, which differs from the previous report [9] where the linear behavior is realized at the whole temperature region. Because the Curie temperature of 103 K in Ref. [9] is quite lower than that of our sample, the sample quality would make a difference in the Arrott plots.

Generally, the spontaneous magnetization $M_0(T)$, the reciprocal susceptibility $1/\chi(T)$, and the Curie temperature T_C can be obtained from the Arrott plots. The spontaneous magnetization and the reciprocal susceptibility can be estimated from intercepts of linear extrapolation of the Arrott plots. In the present case, the Arrott plots show concave curvatures around T_C. According to Takahashi's theory of spin fluctuations for a weak itinerant ferromagnet [12], the M^2 and M^4 terms vanish and the M^6 term remains at T_C, leading to a linear relationship of M^4 and H/M consistent with the present experimental observation. Then we can determine T_C by M^4 vs H/M plots as shown in Fig. 1(b).

The temperature dependence of $M_0(T)$ and $1/\chi(T)$ are shown in Fig. 2. The spontaneous magnetization at 2 K is found to be 0.46 μ_B/Co and the Curie temperature to be 133 K, which is almost equal to the previously reported value [15]. In the case of $H \parallel c$, the c-axis component of the spontaneous magnetization seems to be zero because of the ab-plane alignment of the ferromagnetic moment. As shown in M vs H plots at the high-field region in the insets of Figs. 1(a) and 1(c), there is not much difference between the magnetizations with $H \parallel a$ and with $H \parallel c$. The reciprocal susceptibility with $H \parallel a$ in the high-temperature region obeys the Curie-Weiss law and the one with $H \parallel c$ follows a modified

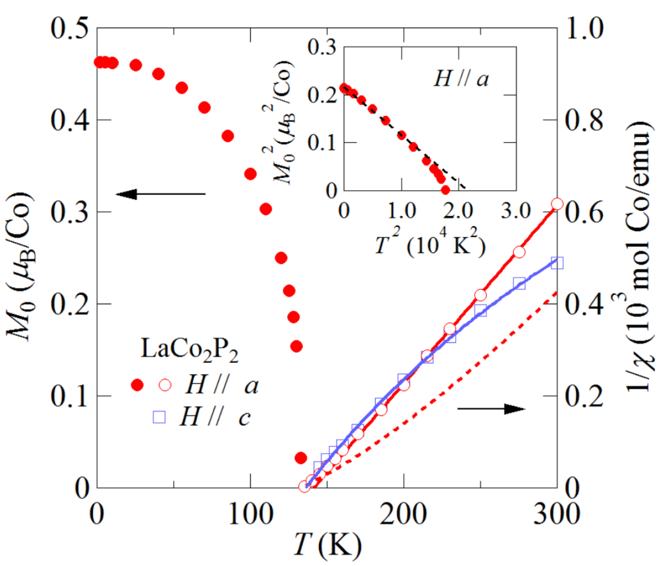

FIG. 2. (Color online) Temperature dependence of spontaneous magnetization $M_0(T)$ and reciprocal susceptibility $1/\chi(T)$ of $LaCo_2P_2$. Closed circles indicate M_0 for $H \parallel a$. Open circles and squares indicate $1/\chi$ for $H \parallel a$ and $H \parallel c$, respectively. The solid lines are the fitting curve by the Curie-Weiss law with finite χ_0. The dashed line is a calculated curve according to self-consistent renormalization theory for spin fluctuations. Inset: M_0^2 for $H \parallel a$ plotted against T^2.

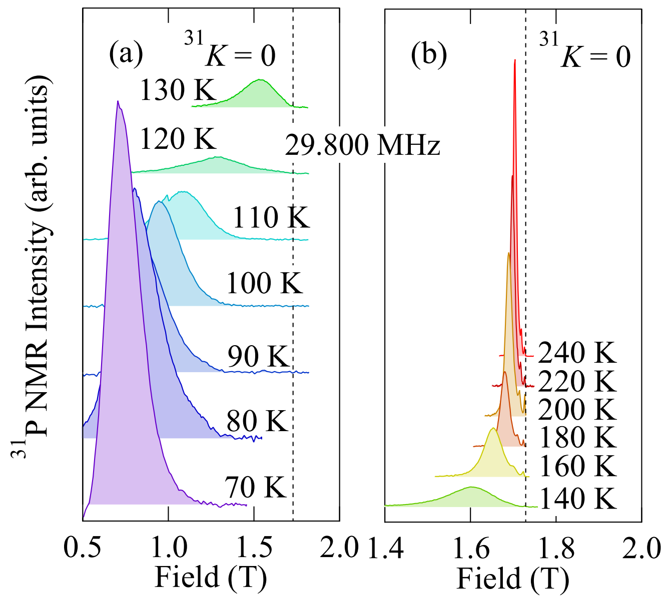

FIG. 3. (Color online) Field-swept ^{31}P NMR spectra of the c-axis-aligned powder sample of $LaCo_2P_2$ below T_C (A) and above T_C (B). Dashed lines in each panel indicate the resonance field with $^{31}K = 0$.

Curie-Weiss law with the temperature-independent term χ_0. Therefore the $\chi_{H\parallel c}$ is somewhat larger than $\chi_{H\parallel a}$ at room temperature, and then the magnitude relation of χ is reversed in the low temperatures. The derived effective magnetic moment per Co atom has little anisotropy and its values are 1.44 μ_B/Co in $H \parallel a$ and 1.37 μ_B/Co in $H \parallel c$. The ratio of the effective magnetic moment $p_{\rm eff}$ and spontaneous magnetic moment p_s is $1.44/0.46 = 3.13$. The value larger than 1 is typical of itinerant ferromagnetic compounds.

Figure 3 shows field-swept NMR spectra of the c-axis-aligned powder sample of $LaCo_2P_2$ measured in a constant frequency of 29.800 MHz. All spectra show a single peak without any fine structures, indicating that the powder is well aligned. As temperature decreases, the peak shifts to a lower field and the spectrum width becomes larger, especially below T_C. Such behaviors can be due to the effects of the increase in magnetization. All other field-swept and constant field spectra (not shown in Fig. 3) also have a single peak structure. The shift is determined from the center of the peak.

Figure 4 shows the temperature dependence of the Knight shift. The Knight shift of the c-axis-aligned powder sample and the single crystals with $H \parallel c$ are almost the same, supporting that our measurements of single crystals are not affected by eddy current heating.

As shown in Fig. 4, the Knight shift with $H \parallel a$ is larger than that with $H \parallel c$. It is probably due to the difference of the hyperfine coupling constant in each field direction to compare between χ and K. Figure 5 shows the K-H/M plots, in which the shift is plotted against H/M with temperature as an implicit parameter. Since the Knight shift corresponds to the local susceptibility at each nuclear site in the paramagnetic region, the K-H/M plot shows linearity with a correlation coefficient corresponding to a hyperfine coupling constant. In the case of $LaCo_2P_2$, all the nondiagonal elements of the

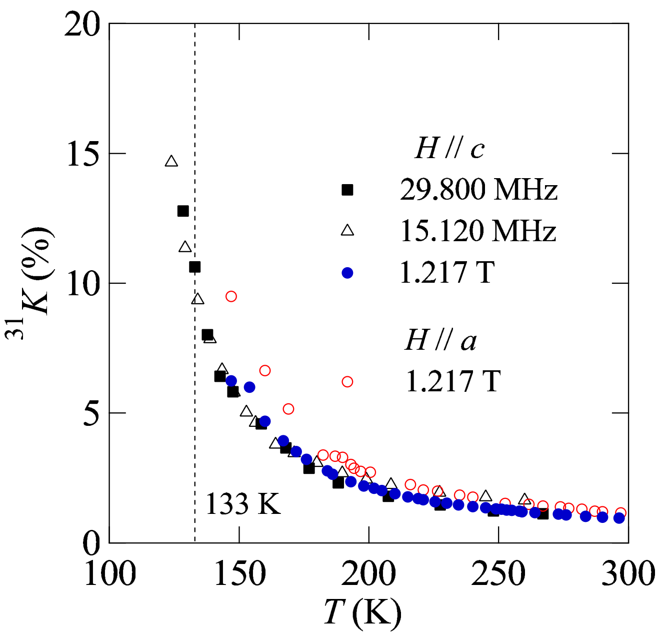

FIG. 4. (Color online) Temperature-dependent shift ^{31}K. Closed squares and open triangles indicate ^{31}K of the c-axis-aligned powder sample with frequencies 15.120 and 29.800 MHz, respectively. Closed and open circles indicate ^{31}K of the single crystals under the applied field 1.217 T, with the field parallel to the c-axis and a-axis, respectively. Dashed lines indicate the Curie temperature $T_C = 133$ K.

hyperfine coupling tensor are zero because of the symmetry of the P site. As shown in Fig. 4(b), the linearity of the K-H/M plots holds above T_C, and the diagonal components of the hyperfine coupling tensor are estimated as follows: $A_a^{hf} = 3.21\ \mathrm{T}/\mu_B$ and $A_c^{hf} = 2.62\ \mathrm{T}/\mu_B$ in single crystals and $A_c^{hf} = 2.27\ \mathrm{T}/\mu_B$ in the c-axis-aligned sample. Because of the difficulty of estimating the absolute value of magnetic

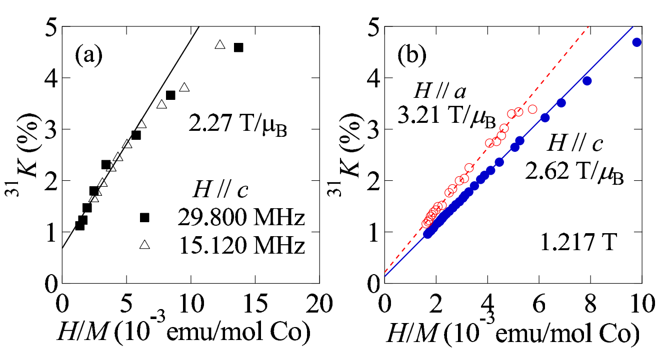

FIG. 5. (Color online) Shift ^{31}K versus M/H plots constructed with the temperature as an implicit parameter. (a) Field-sweep measurements of the c-axis-aligned powder sample with frequencies 15.120 MHz (closed squares) and 29.800 MHz (open triangles). The solid line indicates the results of linear fitting to the data between 170 and 260 K. (b) FT-NMR measurements of the single crystals under the applied field 1.217 T, with the field parallel to the a axis (open circles) and c axis (closed circles). The solid and dashed lines indicate the results of linear fitting to the data between 160 and 300 K for $H \parallel a$ and $H \parallel c$, respectively.

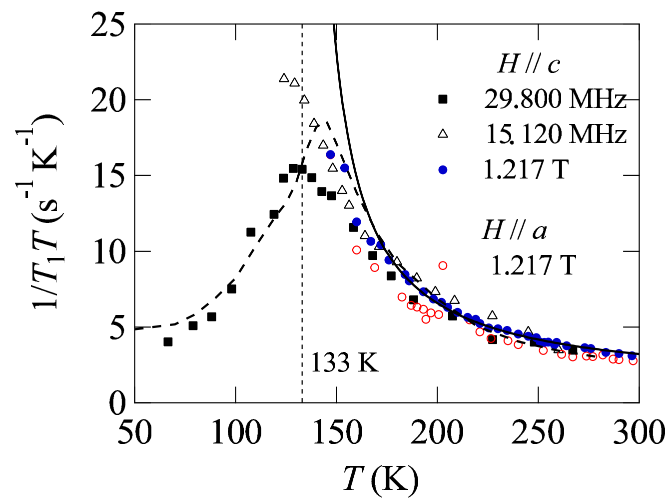

FIG. 6. (Color online) Temperature dependence of $1/T_1T$. Closed squares and open triangles indicate $1/T_1T$ of the c-axis-aligned powder sample with frequencies 15.120 and 29.800 MHz, respectively. Closed and open circles indicate $1/T_1T$ of the single crystals under the applied field 1.217 T, with the field parallel to the c-axis and a-axis, respectively. The solid and dashed lines are the fitting curve by the modified Curie-Weiss law $1/T_1T = \mathrm{const.} + \frac{C}{T-T_C}$ and by the finite field model $1/T_1T = \mathrm{const.} + \frac{bM/H}{1+AM^3/H}$, respectively.

susceptibility of the c-axis-aligned sample fixed in epoxy, we use the susceptibility of single crystals, causing the difference of A_c^{hf}. Therefore the value of single crystals is adopted. The isotropic and anisotropic hyperfine coupling constants are calculated as $A_{iso}^{hf} = (A_c^{hf} + 2A_a^{hf})/3 = 3.02\ \mathrm{T}/\mu_B$ and $A_{ani}^{hf} = (A_c^{hf} - A_a^{hf})/3 = -0.20\ \mathrm{T}/\mu_B$, respectively. A tendency of A_a^{hf} larger than A_c^{hf} was found in other $ThCr_2Sr_2$-type pnictides, i.e., $BaFe_2As_2$ [16] and $SrCo_2As_2$ [17]. The local structure in which the transition metal is tetrahedrally coordinated by Pn is dominantly effective in the hyperfine coupling constant.

Next, we discuss the dynamical magnetic properties through the nuclear-spin-lattice relaxation rate $1/T_1$. Figure 6 shows the temperature dependence of $1/T_1T$ measured at conditions written in the figure caption. The value of $1/T_1T$ increases with cooling to T_C from room temperature and takes a maximum at T_C. In the high-temperature region, $1/T_1T$ shows Curie-Weiss behavior: $1/T_1T = 0.95 + 376/(T - 133)$. In the case of a magnetic transition, $1/T_1T$ ordinary shows divergent behavior due to the divergence of the dynamical susceptibility. Because the divergent behavior is suppressed by an applied field, $1/T_1T$ with constant frequency 29.800 MHz is smaller near T_C and it is roughly reproduced by the equation $1/T_1T = 0.95 + (7 \times 10^6 M/H)/(1 + 0.3M^3/H)$, where M and H are units of emu/mol and Oe, respectively [18]. The $1/T_1T$ reflects the wave-vector $\boldsymbol{q}$ summation of the field-vertical component of the imaginary part of the dynamical electron spin susceptibility $\chi(\boldsymbol{q},\omega)$, which is described as

$$(1/T_1T)_\alpha = 2 \cdot \gamma_N \sum_{\beta\perp\alpha} \sum_q [A_\beta^{hf}(\boldsymbol{q})]^2 \frac{\mathrm{Im}\chi_\beta(\boldsymbol{q},\omega_0)}{\omega_0}, \quad (1)$$

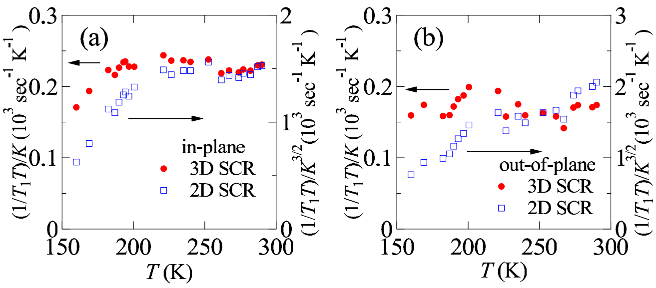

FIG. 7. (Color online) Temperature dependence of $1/T_1TK$ (closed circles) and $1/T_1TK^{1.5}$ (open squares). (a) In-plane data are calculated from $(1/T_1T)_c$ and K_a. (b) Out-of-plane data are calculated from $2(1/T_1T)_a - (1/T_1T)_c$ and K_c.

where γ_N, $A_\beta^{\rm hf}(\boldsymbol{q})$, and ω_0 are the gyromagnetic ratio of nuclei, $\boldsymbol{q}$-dependent hyperfine coupling constant, and the NMR resonance frequency, respectively. In the present case, the transferred hyperfine fields contribute dominantly because the hyperfine field is large, which cannot be explained by only the dipole-dipole interactions. It suggests that the hyperfine interaction is limited in a local area, causing small $\boldsymbol{q}$ dependence. We assume the relation of $A_\beta^{\rm hf}(\boldsymbol{q}) = A_\beta^{\rm hf}(0)$ for simplicity. We introduce the in-plane component of spin fluctuations $(1/T_1T)_{\rm in} = (1/T_1T)_c$ and the out-of-plane component $(1/T_1T)_{\rm out} = 2(1/T_1T)_a - (1/T_1T)_c$. In the framework of the SCR theory of spin fluctuations, we can evaluate the parameters of spin fluctuations. The SCR theory predicts that $1/T_1T$ has a linear relation with $\chi(0)$ in three-dimensional (3D) systems and with $\chi(0)^{1.5}$ in two-dimensional (2D) systems [19]. We plotted $(1/T_1T)_{\rm in(out)}$ against $K_{a(c)}$ and $K_{a(c)}^{1.5}$, and estimated the d-spin part from the equation $(1/T_1T)(T) = (1/T_1T)_d(T)K_d^n(T) + \text{const}$, $n = 1, 1.5$.

Plots of $(1/T_1T)_d/K_d$ and $(1/T_1T)_d/K_d^{1.5}$ against temperature are shown in Fig. 7. Above 220 K, the in-plane data can be explained by the 2D relation slightly better than by that of 3D relation. Below 220 K, the 2D relation breaks down. It is difficult to determine the dimensionality of the ferromagnetic fluctuations in $LaCo_2P_2$ from only $1/T_1T$ data. Therefore we evaluate spin-fluctuation parameters and discuss comprehensively whether they are 2D or 3D. In the case of a 3D model with ferromagnetic fluctuations, spin-fluctuation parameters can be obtained by the following equations:

$$(1/T_1T)/K = (1/T_1T)/(A^{\rm hf}\chi) = \frac{3\gamma_n^2 A^{\rm hf}}{4\pi T_0}, \quad (2)$$

$$T_{\rm C} = (60c)^{-3/4} p_{\rm s}^{3/2} T_{\rm A}^{3/4} T_0^{1/4} \quad (c = 0.335\,3), \quad (3)$$

where $p_{\rm s}$ is the spontaneous magnetization at 0 K, and T_0 and $T_{\rm A}$ are the energy width of the dynamical spin-fluctuation spectrum and the dispersion of the static magnetic susceptibility in the wave vector $\boldsymbol{q}$ space, respectively. In the case of itinerant ferromagnets, we can also estimate the parameters from the static magnetization by using Takahashi's theory, which is developed from the SCR theory by assuming a conservation of the total amplitude of sum of zero point and thermal spin fluctuations against temperature [12]. Moreover, $T_{\rm A}$ can be independently estimated from an M^4 vs H/M curve at $T_{\rm C}$ and M_0^2 vs T^2 plot from the following equations:

$$M^4 = 1.17 \times 10^{18}\left(T_{\rm C}^2/T_{\rm A}^3\right)H/M, \quad (4)$$

$$\left(\frac{M_0(T)}{M_0(0)}\right)^2 = 1 - \frac{50.4}{p_{\rm s}^4}\left(\frac{T}{T_{\rm A}}\right)^2, \quad (5)$$

where M and H are units of emu/mol and Oe, respectively. The obtained value of $T_{\rm A}$ from Eq. (4) is 6480 K, which is consistent with the values estimated from the Arrott plot at 2 K [14]. The value of $T_{\rm A}$ from Eq. (4) is 4850 K and is smaller than the values from other equations but is of reasonable magnitude. Here, we defined $T_{\rm A}^*$ as $T_{\rm A}$ estimated from Eq. (4).

In the case of 2D ferromagnetic fluctuations, spin-fluctuation parameters show the following relation:

$$(1/T_1T)/K^{1.5} = (1/T_1T)/(A^{\rm hf}\chi)^{1.5} = \frac{\gamma_n^2\sqrt{A^{\rm hf}}\sqrt{T_{\rm A}}}{\sqrt{2}T_0}. \quad (6)$$

Since the relationship corresponding to Eq. (3) is unknown in the 2D case, T_0 and $T_{\rm A}$ cannot be determined uniquely.

We obtained spin-fluctuation parameters from the NMR and magnetization data as shown in Table I. There is slight difference of T_0 between in-plane and out-of-plane NMR results, suggesting that $LaCo_2P_2$ has almost isotropic three-dimensional spin fluctuations. In our preliminary ^{31}P NMR study of a nearly ferromagnet $SrCo_2P_2$, a ratio of T_0 of in-plane and out-of-plane $T_0^{\rm in}/T_0^{\rm out}$ is 2.8 and its ferromagnetic interactions are 2D-like rather than 3D. The dimensionality of the ferromagnetic interactions is one of the important factors for the difference in the ground state in the two compounds. The three-dimensional interaction in $LaCo_2P_2$ stabilizes the ferromagnetic orderings.

In addition, we can check the consistency of T_0 and $T_{\rm A}^*$ estimated from static magnetizations with Takahashi's theory. The above results support that ferromagnetic interactions of $LaCo_2P_2$ are 3D and also support Takahashi's assumption with the conservation of the total amplitude. The temperature dependence of reciprocal susceptibility $1/\chi(T)$ in the paramagnetic region can be calculated using spin-fluctuation parameters according to SCR theory. The calculated $1/\chi(T)$

TABLE I. Magnetic and spin-fluctuation parameters of $LaCo_2P_2$. The spontaneous magnetization $p_{\rm s}$ and the effective Bohr magneton number $p_{\rm eff}$ are estimated from the magnetization data. Spin-fluctuation parameters T_0, $T_{\rm A}$, and $T_{\rm A}^*$ are estimated both from the magnetization data with Takahashi's theory and from NMR results with SCR theory.

Reference data	Theory	Dimension	$p_{\rm s}$	$p_{\rm eff}$	$T_{\rm C}$ (K)	T_0 (K)	$T_{\rm A}$ (K)	$T_{\rm A}^*$(K)
NMR (in-plane)	SCR	3D	0.463	1.44	133	890	6.48×10^3	-
NMR (out-of-plane)	SCR	3D	0.463	1.44	133	928	6.62×10^3	-
Magnetization [14]	Takahashi	3D	0.463	1.44	133	914	6.58×10^3	6.41×10^3

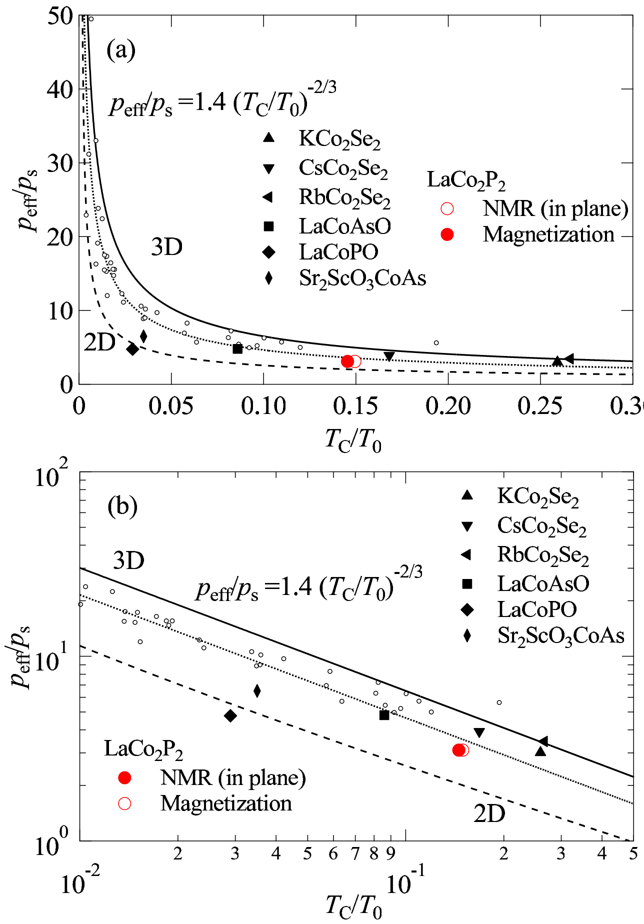

FIG. 8. (Color online) (a) Generalized Rhodes-Wohlfarth plot. (b) Deguch-Takahashi plot. Closed and open circles show the value in $LaCo_2P_2$ estimated from NMR and magnetization data, respectively. Triangles and squares show the values of ferromagnets with quasi-two-dimensional Co layers in Refs. [22–25]. Solid and dashed lines are the theoretical relation between p_{eff}/p_s and T_C/T_0 for 3D and 2D ferromagnetic systems, respectively. The small circles are data reproduced from Refs. [21,26–34].

shows small deviations as shown in Fig. 2, while its slope at high temperatures, which is associated with the effective Bohr magneton number p_{eff}, shows a good agreement with experimental results with $H \parallel a$. Thus evaluated spin-fluctuation parameters are appropriate values.

In accordance with Takahashi's theory, the ratios of p_{eff}/p_s and T_C/T_0 are important for a characterization of itinerant ferromagnets and satisfy the generalized Rhodes-Wohlfarth relation $p_{eff}/p_s = 1.4(T_C/T_0)^{-2/3}$ in the 3D system. For weak ferromagnetic compounds, p_{eff}/p_s is large and T_C/T_0 is small because of its large spin fluctuations. Both p_{eff}/p_s and T_C/T_0 approach to 1 along with the generalized Rhodes-Wohlfarth relation as the spin fluctuations become small. It should be noted that T_0 corresponds to the spectral width in frequency space at $q = Q$ ($Q = 0$ in the ferromagnetic case), and a large T_0 value means large longitudinal spin fluctuations. Figure 8 shows the generalized Rhodes-Wohlfarth plot and its log-log plot. In addition to the generalized Rhodes-Wohlfarth relation, we drew the theoretical line for the quasi-2D spin-fluctuations system [20]. The present data and other data of itinerant ferromagnets with quasi-2D Co layers are roughly located along $p_{eff}/p_s = 1.4(T_C/T_0)^{-2/3}$, where the proportionality factor has a width [12,21]. In comparison with each cobalt compound, p_{eff}/p_s reaches almost the same value, though, T_C/T_0 in LaCoPO and Sr_2ScO_3CoAs, where the distance between tetrahedral Co*Pn* layers is relatively long, is smaller than that of $ThCr_2Si_2$-type compounds. As shown in Fig. 8, the data of LaCoAsO [22], LaCoPO [23], and Sr_2ScO_3CoAs [24] are located closer to the theoretical line in 2D systems than in 3D. The data of $LaCo_2P_2$ is located between the theoretical line in a 3D system and that in a 2D system. With totally considering the analyzed results of the NMR data and static magnetization, the system has three-dimensionality. Small anisotropy, however, may induce the estrangement from the theoretical line in 3D systems. Although we succeeded in qualitative and rough quantitative characterization of spin fluctuations of $LaCo_2P_2$, it is difficult to quantitatively explain exactly the ferromagnetic properties, including low dimensionality, and that is a future issue to be addressed.

IV. CONCLUSION

We clarified the microscopic magnetic properties of $LaCo_2P_2$ by using ^{31}P NMR measurements. We evaluated the spin-fluctuation parameter from a $1/T_1T$ vs K plot by using SCR theory. Both in-plane and out-of-plane parameters T_0 show almost the same value, indicating that the system has nearly isotropic three-dimensional spin fluctuations. Though $LaCo_2P_2$ has quasi-two-dimensional CoP layers and shows highly magnetic anisotropy in the ferromagnetic region, its spin fluctuations have a three-dimensional character in the paramagnetic region and can be understood in the frameworks of the SCR theory and Takahashi's theory of spin fluctuations.

ACKNOWLEDGMENTS

This work is supported by Grants-in-Aid for Scientific Research (Grants No. 22350029 and No. 26410089) from the Ministry of Education, Culture, Sports, Science and Technology of Japan.

[1] M. Rotter, M. Tegel, and D. Johrendt, Phys. Rev. Lett. **101**, 107006 (2008).

[2] E. Mörsen, B. D. Mosel, W. Müller-Warmuth, M. Reehuis, and W. Jeitschko, J. Phys. Chem. Solids **49**, 785 (1988)

[3] M. Reehuis and W. Jeitschko, J. Phys. Chem. Solids **51**, 961 (1990).

[4] F. Ronning, E. D. Bauer, T. Park, S.-H. Baek, H. Sakai, and J. D. Thompson, Phys. Rev. B **79**, 134507 (2009).

[5] C. de la Cruz *et al.*, Nature (London) **453**, 899 (2008).

[6] F. L. Ning, K. Ahilan, T. Imai, A. S. Sefat, M. A. McGuire, B. C. Sales, D. Mandrus, P. Cheng, B. Shen, and H.-H. Wen, Phys. Rev. Lett. **104**, 037001 (2010).

[7] E. Dagotto, Rev. Mod. Phys. **66**, 763 (1994).

[8] G. R. Stewart, Rev. Mod. Phys. **73**, 797 (2001).

[9] M. Reehuis, C. Ritter, R. Ballou, and W. Jeitschko, J. Magn. Magn. Mater. **138**, 85 (1994).

[10] M. Reehuis, W. Jeitschko, G. Kotzyba, B. Zimmer, and X. Hu, J. Alloys Compd. **266**, 54 (1998).

[11] M. Imai, C. Michioka, H. Ohta, A. Matsuo, K. Kindo, H. Ueda, and K. Yoshimura, Phys. Rev. B **90**, 014407 (2014).

[12] Y. Takahashi, J. Phys. Soc. Jpn. **55**, 3553 (1986).

[13] T. Moriya, J. Magn. Magn. Mater. **100**, 261 (1991).

[14] M. Imai, C. Michioka, H. Ueda, H. Ohta, and K. Yoshimura, J. Jpn. Soc. Powder Powder Metall. **61.S1**, S60 (2014).

[15] C. M. Thompson, A. A. Arico, K. Kovnir, and M. Shatruk, J. Appl. Phys. **107**, 09E316 (2010).

[16] K. Kitagawa, N. Katayama, K. Ohgushi, M. Yoshida, and M. Takigawa, J. Phys. Soc. Jpn. **77**, 114709 (2008).

[17] A. Pandey, D. G. Quirinale, W. Jayasekara, A. Sapkota, M. G. Kim, R. S. Dhaka, Y. Lee, T. W. Heitmann, P. W. Stephens, V. Ogloblichev, A. Kreyssig, R. J. McQueeney, A. I. Goldman, A. Kaminski, B. N. Harmon, Y. Furukawa, and D. C. Johnston, Phys. Rev. B **88**, 014526 (2013).

[18] M. Kontani, T. Hioki, and Y. Masuda, Solid State Commun. **18**, 1251 (1976).

[19] M. Hatatani and T. Moriya, J. Phys. Soc. Jpn. **64**, 3434 (1995).

[20] Y. Takahashi, J. Phys.: Condens. Matter **9**, 10359 (1997).

[21] K. Yoshimura, M. Takigawa, Y. Takahashi, H. Yasuoka, and Y. Nakamura, J. Phys. Soc. Jpn. **56**, 1138 (1987).

[22] H. Ohta and K. Yoshimura, Phys. Rev. B **79**, 184407 (2009).

[23] H. Sugawara, K. Ishida, Y. Nakai, H. Yanagi, T. Kamiya, Y. Kamihara, M. Hirano, and H. Hosono, J. Phys. Soc. Jpn. **78**, 113705 (2009).

[24] H. Ohta, D. Noguchi, K. Nabetani, and H. A. Katori, Phys. Rev. B **88**, 094441 (2013).

[25] J. Yang, B. Chen, H. Wang, Q. Mao, M. Imai, K. Yoshimura, and M. Fang, Phys. Rev. B **88**, 064406 (2013).

[26] D. Bloch, J. Voiron, V. Jaccarino, and J. H. Wernick, Phys. Lett. A **51**, 259 (1975).

[27] F. R. Deboer, C. J. Schinkel, J. Biesterbos, and S. Proost, J. Appl. Phys. **40**, 1049 (1969).

[28] J. Takeuchi and Y. Masuda, J. Phys. Soc. Jpn. **46**, 468 (1979).

[29] S. Ogawa, J. Phys. Soc. Jpn. **40**, 1007 (1976).

[30] S. Ogawa, J. Phys. Soc. Jpn. **25**, 109 (1968).

[31] K. Shimizu, H. Maruyama, H. Yamazaki, and H. Watanabe, J. Phys. Soc. Jpn. **59**, 305 (1990).

[32] J. Beille, D. Bloch, and M. J. Besnus, J. Phys. F: Met. Phys. **4**, 1275 (1974).

[33] R. Nakabayashi, Y. Tazuke, and S. Murayama, J. Phys. Soc. Jpn. **61**, 774 (1992).

[34] A. Fujita, K. Fukamichi, H. A. Katori, and T. Goto, J. Phys.: Condens. Matter **7**, 401 (1995).